ISBN: 978-3-95450-245-5 ISSN: 2226-0374 doi:10.18429/JACoW-COOL2023-MOPPM1R3

# SPECIFICATIONS AND STATUS OF THE NEW ELECTRON COOLER FOR THE CERN ANTIPROTON DECELERATOR (AD)

A. Rossi*, C. Accettura, W. Andreazza, A. Bollazzi, C. Castro Sequeiro, J. Cenede, N. Chritin, Y. Coutron, A. Frassier, G. Khatri, D. Gamba, L. Joergensen, C. Machado, O. Marqversen, L. Ponce, A. Pikin, J. A. Ferreira Somoza, M. Sameed, Y. Thurel, A. Sinturel, T. Todorcevic, G. Tranquille, L. von Freeden, CERN, Geneva, Switzerland

*Abstract*

A new electron cooler for the Antiproton Decelerator (AD) is being designed at CERN, and will replace the current device (in operation for more than 40 years), during the next Long Shutdown (2026-2028). The functional specifications, recalled in this paper, favour high reliability, with improved performance in terms of time of cooling, obtained mainly with better field quality and possibly higher electron beam current. The status of the new electron cooler design is presented, showing an evolution that aims at easing integration, installation and maintenance.

## INTRODUCTION

The AD (Antiproton Decelerator) ring decelerates antiprotons ($\bar{p}$) from 3.5 GeV/c to 100 MeV/c which are then injected into the ELENA (Extra Low ENergy Antiproton) ring. To counteract beam blow up during deceleration, stochastic cooling and electron cooling are carried out during the AD cycle, with electron cooling operating at 300 and 100 MeV/c momentum of the circulating beam [1]. While the AD ring has been operating since the year 2000, the current electron cooler is around 40 years old, being recovered from the Low Energy Antiproton Ring (1982-1997) [2]. The magnets are even older and the companies who produced them no longer exist. A replacement for the electron cooler is therefore envisaged, in the frame of the Consolidation Project at CERN. The new device aims at a high reliability, by design and robustness of the ancillary equipment. Moreover, it is expected to have improved performance in terms of time of cooling, mainly obtained by limiting the electron transverse and longitudinal temperature and switching on/off the electron beam during the energy ramps, as described in the following. In this paper we give the main parameters of design of the new cooler, explaining the technical choices implemented as an evolution of what was presented in [3]. A brief overview of planning for installation will also be given.

## SPECIFICATIONS FOR THE NEW ELECTRON COOLER

The specifications [4] for the new electron cooler are listed in Table 1 where the main design parameters are compared to the one of the presently installed electron cooler, with blue font highlighting the main differences. The cooling will act at the same momentum plateaux as for the current AD cycle,

Table 1: Main Parameters of the Present and New E-Cooler

| | **Present** | **This Spec.** |
|---|---|---|
| **Gun:** | | |
| Magnetic field [T] | 0.06 | 0.24 † |
| Perveance [$\mu AV^{2/3}$] | 0.58 | 2.5 |
| Cathode radius [mm] | 25 | 12.5 |
| **Toroid:** | | |
| Magnetic field [T] | 0.06 | 0.06 |
| Angle $\phi_0$ [rad] | 0.6283 | 0.6283 |
| Radius $r_{tor}$ [m] | 1.133 | 1.133 |
| Integrated $\perp$ field [T·m] | ~ 0.016 | $\lesssim$ 0.016 |
| **Cooling region:** | | |
| Vacuum pressure [mbar] | ~ $10^{-10}$ | < $10^{-10}$ |
| Length [m] | < 1 | ~ 1 |
| Radius [mm] | 25 | ≥ 25 |
| Magnetic field [T] | 0.06 | 0.06 |
| $(B_\perp/B_\parallel)_{max}$ | $10^{-3}$ | $10^{-4}$ |
| $(B_\perp/B_\parallel)_{rms}$ | n.a. | < $10^{-4}$ |
| $e^-\ k_BT_\perp$ [meV] | 100 | $\lesssim$ 100 |
| $e^-\ k_BT_\parallel$ [meV] | — | $\lesssim$ 1 |
| $r_{\text{e-beam}}$ [mm] | — | up to 25 |
| $E_{e^-}$ [keV] | 2.9 100 MeV/c<br>25.5 300 MeV/c | 2.9 100 MeV/c<br>25.5 300 MeV/c |
| $E_{e^-}$ resolution [eV] | 1 | 0.1 2.9 keV<br>1 25.5 keV |
| $E_{e^-}$ stability [eV] | — | < 0.1 2.9 keV<br>< 1 25.5 keV |
| $e^-$ current $I_0$ [A] | 2.4 | 2.4 nominal<br>4.8 ultimate |
| Stability [$\Delta I/I_0$] | — | ~ $10^{-4}$ |
| Relative losses [$\delta I/I_0$] | — | < $10^{-4}$ |
| Max time to vary from 25.5 keV to 2.9 keV [s] | > 5 | ~ 1 |
| $e^-$ beam start/stop [s] | — | ≪ 1 |
| BPM relative $e^-/\bar{p}$ accuracy [μm] | — | $\lesssim$ 100 |
| E-cooler availability | — | 99% |

† The main differences are highlighted in blue in the text

i.e. 300 and 100 MeV/c momentum of the circulating beam. In designing the new electron cooler, we tried to improve its performance and reduce the time of cooling, as well as guarantee good reliability. This is approached by trying to limit the transverse and longitudinal electron velocity

* adriana.rossi@cern.ch

ISBN: 978-3-95450-245-5 ISSN: 2226-0374 doi:10.18429/JACoW-COOL2023-MOPPM1R3

spreads, and reduce the angle between $\bar{p}$ and $e^-$ trajectories in the cooling region (see also [4]).

In the following, the technical choices taken to achieve the specified values are detailed.

## TECHNICAL SPECIFICATION AND TYPOLOGY CHOICES

The main technological novelty for the new electron cooler will be the electron gun and collector.

### *Gun, Collector and High Voltage Powering*

The first design for the new electron cooler thermionic gun was presented in [3]. In a thermionic gun the minimum electron transverse temperature at the gun will be determined by the temperature of the cathode, which, for the types of cathode material employed will be around 1000 °C, corresponding to ~0.1 eV. The design is based on simulations [5], showing that a flat cathode geometry would be best to emit as uniformly as possible and with a limited transverse $e^-$ energy as pictured in Fig. 1, which will depend on the magnetic field in which the gun is immersed. The shape of the electrodes was slightly modified (see also [3]), and modelled into COMSOL to check electrostatic and magnetic properties. The final 3D model and prototype are shown in Fig. 2. The estimated perveance of the gun is between 2.2 and 2.5 μA$V^{2/3}$; it follows that to extract 2.4 A (nominal) and 4.8 A (ultimate) electron current —as indicated in Table 1 —the required grid-cathode (see Fig. 2) potential difference ($V_{\text{grid}}$ in Fig. 3) will be ~11 kV and 17 kV, respectively. It should be noted that even if theoretically the time of cooling is inversely proportional to current, in practice electron space-charge and other effects in the cooling region might limit the electron beam transport efficiency and cooling performance, therefore, the optimal current value will be determined experimentally.

The presence of the grid allows to regulate current extraction and $e^-$ velocity independently, and therefore to suppress the beam while ramping the cathode power supply. To reach the required $e^-$ energies (namely 2.9 keV for cooling at 100 MeV/c and 25.5 keV for cooling at 300 MeV/c), the cathode to ground potential ($V_k$ in in Fig. 3) of the present electron cooler is set to 3 kV and 27 kV, respectively. For the new electron cooler the power supply nominal rating is 30 kV. The actual values for operation will be evaluated experimentally. The whole High Voltage system, i.e. grid, collector pot and collector electrodes potentials are referred to the cathode potential, as shown in Fig. 3. This avoids dumping the whole $e^-$ beam power to ground, thereby limiting the size of the power supplies required. Moreover, control of electron losses to ground is automatically done, since if the leakage current is larger than the limit current of the power supply, the HV system will switch off, preventing damage to the vacuum chambers[1]. In the frame of consolidation and reliability improvement, all power supplies in the block diagram of Fig. 3 will be renewed, and provided with spares. The electron energy resolution and stability, and the subsequent requirements imposed upon the powering [6] were taken into account in the selection of the new equipment.

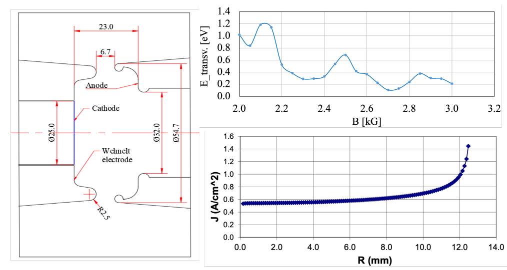


Figure 1: Top: Dependence of maximum transverse electron energy on magnetic field for electron gun with flat cathode and flat electrodes @ $I_{e^-} = 2.5$ A, $E_{e^-} = 27.0$ keV. Bottom: electron gun 2D design and radial distribution of the emission current density for a $r = 12.5$ mm cathode @ $I_{e^-} = 3.5$ A, $V_{\text{grid}} = 12.15$ keV.

As a way to lower the transverse temperature of the electrons, the electron beam is going to be adiabatically expanded [7, 8] by a factor of two. The resulting transverse electron temperature and density after expansion are expected to be $T_\perp = T_{\text{cathode}} \frac{B_{\text{cool}}}{B_{\text{cathode}}}$ and $n_{\text{cool}} = n_{\text{cathode}} \frac{B_{\text{cool}}}{B_{\text{cathode}}}$. Given that in the cooling region the required electron beam radius is 25 mm, and the magnetic field is the same as the one of today's electron cooler, i.e. 0.06 T, this imposes a cathode radius of 12.5 mm and a gun solenoid (called *expansion solenoid*) field intensity of 0.24 T, as $r_{\text{cool}} = r_{\text{cathode}} \sqrt{\frac{B_{\text{cathode}}}{B_{\text{cool}}}}$. The actual cathode will be of 1" diameter (2.54 mm) from Spectra-Mat,Inc.

The gun prototype is presently under test: it passed the vacuum test, with an ultimate vacuum of $5 \times 10^{-8}$ mbar without bake-out; a potential of 27 keV could be applied between both cathode and grid to ground and cathode to grid —with the cathode at room temperature, and no spark or problem was observed. The gun thermal tests, heating the cathode up to nominal and ultimate temperature, are also successfully completed, and the gun is now install in the test stand where current can be extracted and measured. As already described in [8], development for a new collector design started already after a water leak into the vacuum of the present collector. The design was made compatible with the

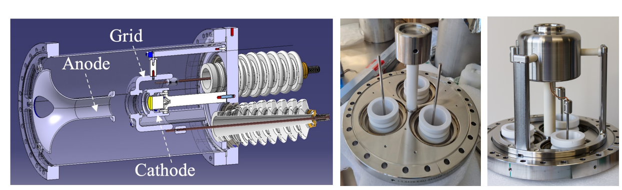


Figure 2: Left h.s.: 3D drawing of the new AD cooler electron gun. Middle: photos of the cathode mounted on the flange, and right: assembly cathode plus gird.

[1] Similarly, other interlocks on magnet cooling water temperature and vacuum will also stop the electron beam and avoid damage.

ISBN: 978-3-95450-245-5 ISSN: 2226-0374 doi:10.18429/JACoW-COOL2023-MOPPM1R3

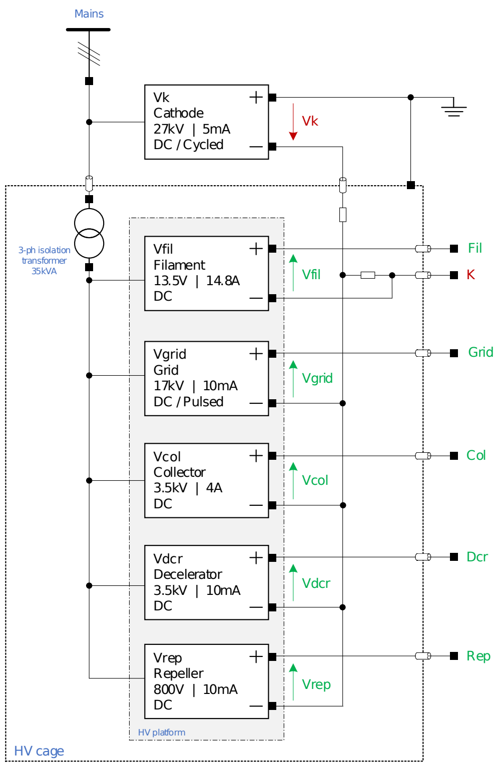


Figure 3: HV powering block diagram.

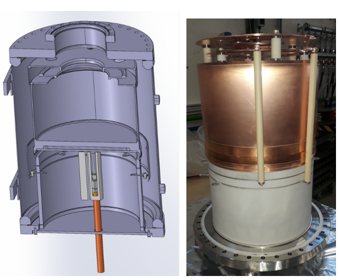

Figure 4: Collector 3D model (left) and prototype (right).

new electron cooler. A picture of the collector 3D design and the prototype built is shown in Fig. 4. The cooling water circuit runs only at the bottom of the collector. The collector features two electrodes, the first to slow down the $e^-$ beam before hitting the collector pot, set at potential $V_{\mathrm{dcr}}$ in Fig. 3 ~ 3 kV difference from the cathode potential, the second to repell electrons that are reflected or desorbed at the collector pot surface, set at a potential $V_{\mathrm{rep}}$ in Fig. 3 close to the cathode potential (only ~800 V difference). This collector has already been tested for several days at 3 kV with a beam of 2 A DC, and the cooling water temperature increased by about 15 °C. Further tests and calculations are to be carried out to validate the design to the maximum power to be absorbed (i.e. 3 kV × 4.8 A).

### *Magnetic System and Powering*

To limit electron temperature heating and improve magnetised cooling time, the field quality in the cooling region solenoid is required to be $\leq 10^{-4}$, a value calculated theoretically [4] and confirmed by experimental evidence by several experts around the world [9], observing a degradation of the cooling time when the field quality was worse than this value. It should be noted that the field quality measured for the present cooling region solenoid, before installation in LEAR, is in the order of $10^{-3}$ [10], which may partially justify why the cooling time at AD is about three times longer than initially foreseen [11]. Two different topologies, depicted in Fig. 5, have been analysed for the new AD cooler design; the first with a full pancake system as in [3] and the second with complete solenoids in the cooling region and the gun and collector arms. A comparison of performance of the two typologies in the cooling region was presented in [12]. The field quality in the pancake system (13 pancake coils) can be tuned by tilting the pancake coil around three pivot points (see Fig. 6; it was found that the system would approach the required field quality if the pancakes were aligned to better than 200 µm. For the complete solenoid the field can be adjusted by regulating the current in the corrector coils (8 horizontal and 8 vertical). Figure 7 shows the magnetic field intensity calculated in the cooling region, for the *perfect* case, and compares to measurements performed for the currently installed electron cooler [10]. A Monte-Carlo analysis was carried out [12] to quantify the field quality expected of the built system. The following assumptions were made:

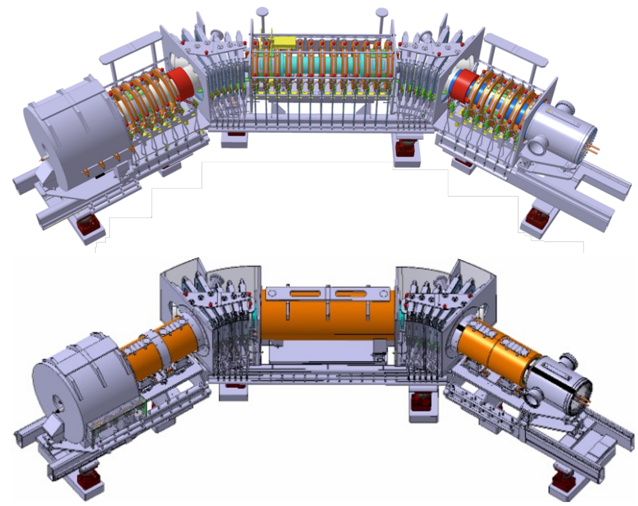

Figure 5: Pancake (top) and complete (bottom) magnetic system design. The ‘complete’ solenoid system has been chosen for the new design.

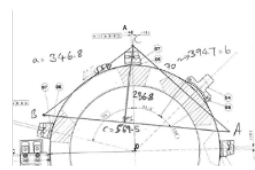

Figure 6: Pancake coil pivot supports.

- The adjustment of each of the three pivot points of the pancakes is normally distributed with $3\sigma = 200$ µm, the

ISBN: 978-3-95450-245-5 ISSN: 2226-0374 doi:10.18429/JACoW-COOL2023-MOPPM1R3



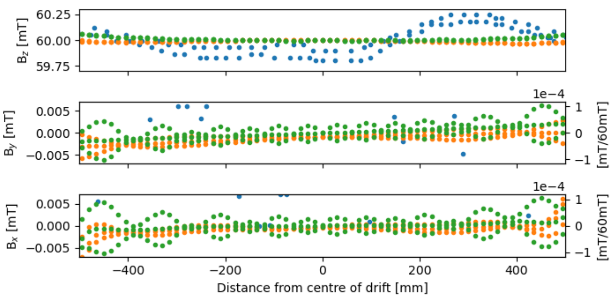


Figure 7: Magnetic field along the direction of motion of the $e^-$ beam ($B_z$), perpendicular to the bending plane ($B_y$) and in the bending plane ($B_x$), estimated in the cooling region for the pancake (orange) and complete (green) typology, for the *perfect* case, i.e. all coils positioned and powered exactly. The values as extracted and scaled for the present magnetic system from [10] are shown in blue, but hardly visible since outside the scale chosen for $B_x$ and $B_y$.

long term stability is normally distributed with $3\sigma$ = 20 µm;

- The current in the corrector coils has a resolution vs. nominal normally distributed with $3\sigma$ = 5 PPM , a ripple of 1 mA RMS, and a long term stability of $3\sigma$ = 1000 PPM.
- Mechanical tolerances should be the same for the pancake and complete solenoid, and therefore are not discussed.

The results show that the two magnet configurations would be expected to give similar performance once built, with a field error of ~ $2 \times 10^{-4}$ due to correction tolerance for the pancake case and ~ $5 \times 10^{-5}$ for the complete case. It was decided to go for the complete cooling region solenoid which features active control of the magnetic field. With the pancake system the main concern was the tight tolerances needed in adjusting the coils position (better than 200 µm) to achieve the required field quality. Besides being tight, the adjustment might be time/resource consuming, and, if any of the pancakes moved or broke during operation, very difficult to reproduce, especially considering that once the cooler is installed it would no longer be possible to measure the magnetic field. As for the magnets in the gun and collector arms, the choice of complete solenoids was made for economical reasons (less costly, especially if the main solenoid is a complete magnet) and for space constraints, to allow the integration of new orbit correctors adjacent to the electron cooler, made necessary by the fact that the new cooler is horizontal and not vertical [3].

The new magnet system is composed of

1. The gun expansion complete solenoid (nominal field 0.24 T, field quality $\lesssim 10^{-3}$), adiabaticity in expansion 0.93 T/m;
2. The arms solenoid (both on the gun and collector side) split in two complete magnets (0.06 T, field quality $\lesssim 10^{-3}$). The arm solenoids closest to the drift are fitted with horizontal and vertical steering coils;
3. The toroid solenoids (0.06 T), formed from 6 coils per side arranged to guarantee as a uniform bending toroidal field as possible, and shape to allow insertion and extraction of the $e^-$ beam into and out of the AD ring; the toroids are also equipped with bending dipole magnets (shaped to match the toroid) to compensate for the residual vertical field from the toroid;
4. The cooling region complete solenoid (0.06 T, field quality $\lesssim 10^{-4}$), equipped with eight horizontal and eight vertical corrector magnets (0.34 mT), plus horizontal and vertical steering magnets to adjust the angle of the electron orbit (0.38 mT);
5. Collector squeeze coil, to compress the $e^-$ beam before the collector entrance.

To optimise procurement time and costs, development work and spares availability, the type of power converters already available at CERN were taken into account when dimensioning the new magnetic system. The layout of the magnet powering is shown in Fig. 8, where almost all parameters have already been fixed. It should be noted that the SMILE type converters for the corrector and steerer magnets are already available as they can be recovered from the present installations and spares that we have at CERN.

### *Vacuum System*

The design of the vacuum system is shown in Fig. 9 and have not significantly changed since [3]. The diameter of the vacuum chamber is everywhere the same as the adjacent chambers in the AD ring (145 mm inner diameter, and round shape). This is an improvement with respect to the present cooler as it provides smoother transition at insertion and extraction of the $e^-$ beam. This also means that the need of clearing electrodes in the toroid chambers (to suppress ions and electrons either created by ionisation of the residual gas or by reflection from the collector) seems unlikely. This aspect is subject to ongoing investigation. The vacuum chambers of the gun and collector arms are identical, but rotated because it was decided to use the same collector design as for the present cooler, with inlet flange of DN150. Vacuum requirements for the new AD cooler impose the coating with NEG wherever possible (for its properties of pumping, low electron stimulated desorption, and to reduce the size of the vacuum chamber and design complexity), the use of NEG strips where the gas load is larger (close to the gun and collector), and the employment of NEXtoor pumps. The average pressure evaluated assuming a secondary electron yield at the collector after one day of operation is estimated to be in the order of ~$5 \times 10^{-10}$ mbar. Without NEG coating, the pressure would be at least an order of magnitude larger [13, 14].

### *Beam Position Monitors — BPM*

One way for speeding the cooling time is to be able to align the $e^-$ and $\bar{p}$ beams to better than 300 µm which translate into a required relative measurement resolution of the BPM reading of $\lesssim$100 µm. The new BPM design, presented in Fig. 10, is estimated to have a resolution of ~90 µm.

ISBN: 978-3-95450-245-5 ISSN: 2226-0374 doi:10.18429/JACoW-COOL2023-MOPPM1R3

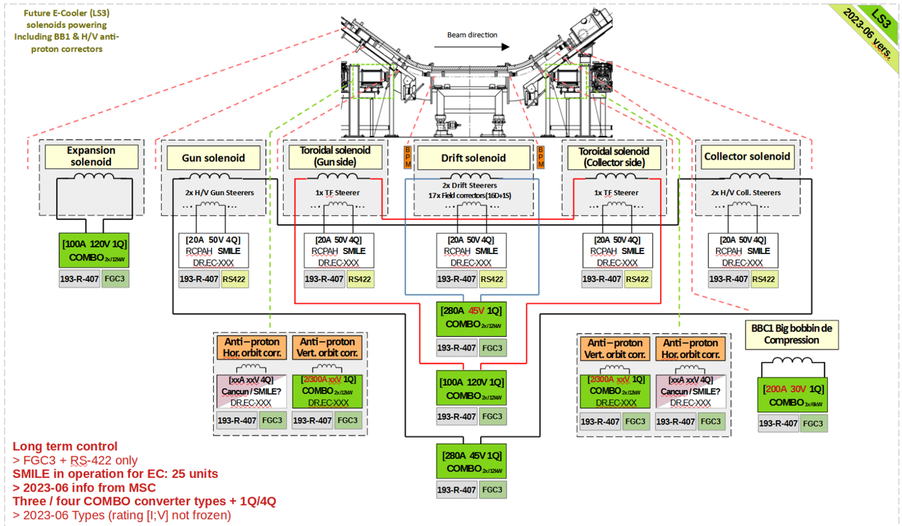


Figure 8: Magnet powering schematics for the new AD cooler.

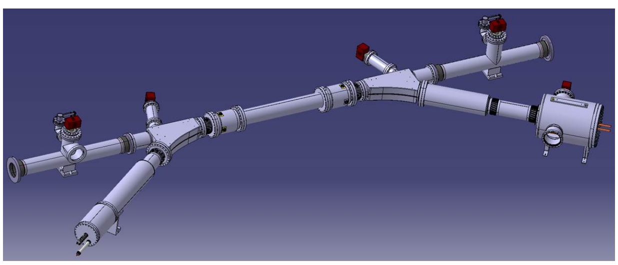

Figure 9: Vacuum chambers for the new electron cooler.

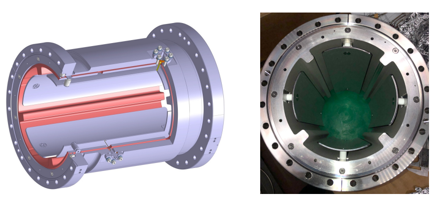

Figure 10: BPM for the new AD cooler.

## TESTING STRATEGY AND SCHEDULE

All components of the new AD electron cooler will be tested separately in the laboratory. Magnets will be tested individually for acceptance and to tune correctors current, plus as an ensemble mounted on the support system to measure steering magnets strength and prepare for operations. Gun and collector are being tested individually, in a straight configuration, with magnets equivalent to those for the final electron cooler. Vacuum chambers and powering system will be tested individually. The magnet powering will be used for the complete magnet test. The de-installation of the current electron cooler will start when all components are proven to work as expected. In the present schedule, this should happen in the second quarter of 2026. After that the new electron cooler will be installed, connected to power, baked and commissioned, with operation to be started after June 2027, i.e. after the end of the Long Shut Down 3 for the CERN injectors.

## CONCLUSION

In this paper the main specification parameters and the newest design of the electron cooler replacing the one installed in the AD ring were presented. The new device aims at improving reliability as well as performance. The magnet design has evolved to complete solenoids which can produce a high quality field with active correction and avoid lengthy and difficult alignment, given the tight requirements. The design is mature and close to completion, and procurement will start in the beginning of year 2024. Provided the testing campaign for all components is successful, the decommissioning of the present electron cooler will start in the second quarter of 2026, and commissioning of the new device in 2027.

## REFERENCES

[1] P. Beloshitsky and T. Eriksson, "The CERN Antiproton Decelerator (AD) operation, progress and plans for the future", presented at the 2nd International Workshop on Atomic Collisions and Atomic Spectroscopy with Slow Antiprotons, Aarhus, Denmark, 14–15 Sep 2001, CERN-OPEN-2002-041, CERN-PS-OP-NOTE-2002-040. `https://cds.cern.ch/record/561996`

[2] G. Tranquille, "Recent highlights from the CERN-AD", *Nucl. Instrum. Meth. A*, vol. 532, pp. 111–117, 2004. `doi:10.1016/j.nima.2004.06.036`

[3] G. Tranquille *et al.*, "A New Electron Cooler for the CERN Antiproton Decelerator (AD)", in *Proc. COOL'21*, Novosibirsk, Russia, Nov. 2021, pp. 95–97. `doi:10.18429/JACoW-COOL2021-P2004`

[4] D. Gamba *et al.*, "Functional Specification for the New AD electron cooler", Rep. AD-LNT-ES-0001, EDMS 2772724, CERN, 2023. `https://edms.cern.ch/document/2772724`

ISBN: 978-3-95450-245-5 ISSN: 2226-0374 doi:10.18429/JACoW-COOL2023-MOPPM1R3

[5] A. Pikin, “Simulations of e-gun for AD e-cooler”, presented at the E-coolers and e-lenses simulations - joint BE-ABP / BE-BI meeting, CERN, Geneva, 10 Jan. 2019. https://indico.cern.ch/event/774322/

[6] C. Machado, “High Voltage powering for the New AD Electron Cooler”, Rep. EDMS 2938278, CERN 2023. https://edms.cern.ch/document/2938278/

[7] H. Danared *et al.*, “Studies of electron cooling with a highly expanded electron beam”, *Nucl. Instrum. Meth. A*, vol. 441, pp. 123–133, 2000. doi:10.1016/S0168-9002(99)01121-3

[8] G. Tranquille, L. Jørgensen, D. Luckin, and R. Warner, “The CERN-ELENA Electron Cooler Magnetic System”, in *Proc. IPAC’18*, Vancouver, BC, Canada, Apr. 4, 2018, pp. 842–845. doi:10.18429/JACoW-IPAC2018-TUPAF056

[9] Discussion at the #12 AD E-Cooler Meeting: AD cooler specs, gun and magnetic system, CERN, 28 Feb. 2023. https://indico.cern.ch/event/1248937/

[10] A. Wolf, L. Hütten, and H. Poth, “Magnetic field measurements for the electron cooling device for LEAR”, Rep. CERN-EP-INT-84-01, CERN, Geneva, 1984.

[11] S. Baird *et al.*, “The anti-proton decelerator: AD”, *Nucl. Instrum. Meth. A*, vol. 391, pp. 210–215, 1997. doi:10.1016/S0168-9002(97)00359-8

[12] L. Von Freeden, presentation at the #12 AD E-Cooler Meeting: AD cooler specs, gun and magnetic system, CERN, 28 Feb. 2023. https://indico.cern.ch/event/1248937/

[13] J.A. Ferreira Somoza, presented at the New AD Electron Cooler Project Review, CERN, Geneva 2022. https://indico.cern.ch/event/1157504/

[14] C. Castro Sequeiro and J.A. Ferreira Somoza, presented at the AD-CONS ELECTRON COOLER PROCUREMENT READINESS REVIEW, CERN, Geneva 28 June 2023. https://indico.cern.ch/event/1298443/